

LETTER TO THE EDITOR

# Hydrogen Balmer line formation in solar flares affected by return currents

J. Štěpán<sup>1,2</sup>, J. Kašparová<sup>1</sup>, M. Karlický<sup>1</sup>, and P. Heinzel<sup>1</sup>

<sup>1</sup> Astronomical Institute, Academy of Sciences of the Czech Republic, v.v.i., Fričova 298, 251 65 Ondřejov, Czech Republic  
e-mail: [stepan;kasparov;karlicky;pheinzel]@asu.cas.cz

<sup>2</sup> LERMA, Observatoire de Paris – Meudon, CNRS UMR 8112, 5, place Jules Janssen, 92195 Meudon Cedex, France  
e-mail: jiri.stepan@obspm.fr

Received 27 June 2007 / Accepted 30 July 2007

## ABSTRACT

**Aims.** We investigate the effect of the electric return currents in solar flares on the profiles of hydrogen Balmer lines. We consider the monoenergetic approximation for the primary beam and runaway model of the neutralizing return current.

**Methods.** Propagation of the 10 keV electron beam from a coronal reconnection site is considered for the semiempirical chromosphere model F1. We estimate the local number density of return current using two approximations for beam energy fluxes between  $4 \times 10^{11}$  and  $1 \times 10^{12}$  erg cm<sup>-2</sup> s<sup>-1</sup>. Inelastic collisions of beam and return-current electrons with hydrogen are included according to their energy distributions, and the hydrogen Balmer line intensities are computed using an NLTE radiative transfer approach.

**Results.** In comparison to traditional NLTE models of solar flares that neglect the return-current effects, we found a significant increase emission in the Balmer line cores due to nonthermal excitation by return current. Contrary to the model without return current, the line shapes are sensitive to a beam flux. It is the result of variation in the return-current energy that is close to the hydrogen excitation thresholds and the density of return-current electrons.

**Key words.** Sun: flares – plasmas – line: formation – atomic processes

## 1. Introduction

The ongoing study of nonthermal excitation of the flaring chromospheric plasmas has been mainly concentrated on the effect of particle beams coming from the coronal reconnection site (Canfield et al. 1984; Hawley & Fisher 1994; Fang et al. 1993; Kašparová & Heinzel 2002; Štěpán et al. 2007, and references therein). However, Karlický & Hénoux (2002) and Karlický et al. (2004) recently suggested that the role of neutralizing return currents can be as important as the role of the primary beam itself, both for intensity and linear polarization profiles. Karlický et al. (2004) proposed a simple model of return current formed by the runaway electrons and compared the rates of atomic transitions due to collisions both with the thermal electrons and with the electrons of the primary beam, and due to collisions with the return current formed by the runaway electrons. They showed that the rates due to the return current would dominate the collisional processes in the atmospheric region of Balmer line formation. However, no calculations of theoretical spectral line profiles were presented.

The aim of this paper is to take a first step towards self-consistent modeling of the Balmer line formation with return-current effects taken into account. We use a semi-empirical model of the flaring atmosphere as a basis for our NLTE radiative transfer model. Then we use a standard model for electron-beam deceleration due to Coulomb collisions with the ambient atmosphere and combine it with the two different physical models of the return-current generation. We incorporate the relevant processes that enter the atomic statistical equilibrium equations and solve them with the non-local equations of radiation transfer. At the end, we discuss the results and validity of our models.

## 2. Electron beam and return-current propagation

We assume an electron beam that is accelerated in a coronal reconnection site and injected into the cold chromosphere along the magnetic field lines. During its propagation, the beam evolves under the influence of several processes (Karlický 1997): (a) the beam generates the return current that decelerates the beam in the return-current electric field, (b) the beam generates the plasma waves causing the quasi-linear relaxation of the beam, and (c) the beam electrons are decelerated and scattered due to collisions with the background plasma particles. In the following model, we neglect the plasma wave processes and the return current is taken in the form of runaway electrons (Rowland & Vlahos 1985; van den Oord 1990; Norman & Smith 1978). In this form, the return-current losses are strongly reduced (Rowland & Vlahos 1985; Karlický et al. 2004). Thus, only collisional losses, as described by Emslie (1978), decelerate the electron beam in our case.

Let  $\Phi = n_B v_B$  be the particle flux of the monoenergetic beam of the energy  $E_B = m_e v_B^2 / 2$ , where  $n_B$  is the density of the beam electrons,  $v_B$  their velocity, and  $m_e$  the mass of the electron. According to Norman & Smith (1978) and Karlický et al. (2004), a fraction of background electrons  $\alpha = n_R / n_e$  forms the current that moves in the opposite direction in order to neutralize the electric current  $e\Phi$  associated with the primary beam. We use  $n_R$  for the number density of the return-current electrons and  $n_e$  for the number density of the background electrons. The neutralization condition can be expressed as

$$en_R v_R = e\Phi. \quad (1)$$

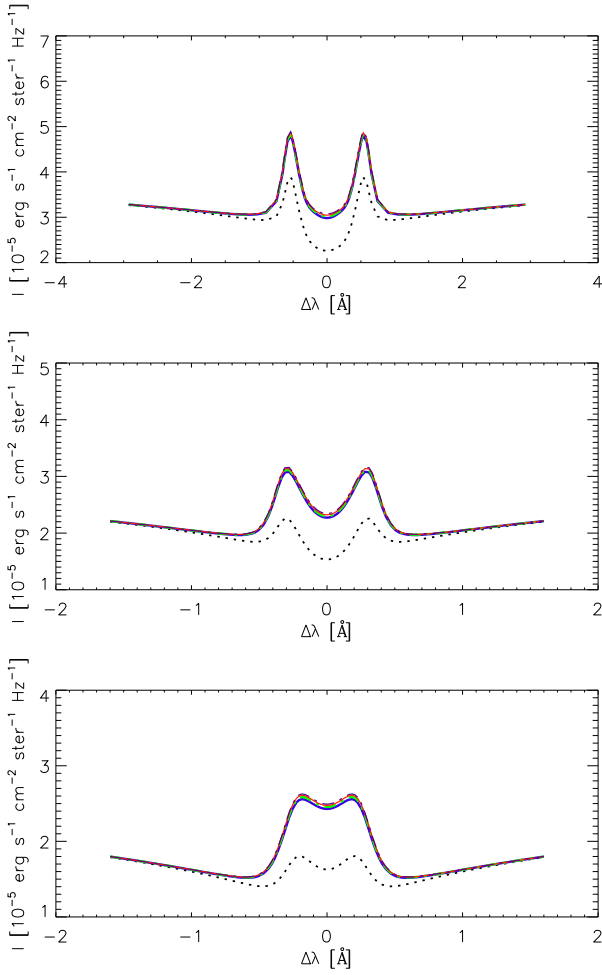


**Fig. 1.** From upper panel: H $\alpha$ , H $\beta$ , and H $\gamma$  disk-center line profiles for  $\mathcal{F}_1 = 0$  (dotted line, black),  $\mathcal{F}_1 = 4 \times 10^{11}$  (thick solid line, blue),  $6 \times 10^{11}$  (thick dash-dotted line, green),  $8 \times 10^{11}$  (thin solid line, red), and  $1.0 \times 10^{12}$  (thin dash-dotted line, violet)  $\text{erg cm}^{-2} \text{s}^{-1}$ . No return-current effects are taken into account. Note that nonthermal profiles almost overlap in this range of beam fluxes.

We assume that all the return-current electrons move with the same superthermal velocity  $v_R$ . Note that the return-current flux only depends on the total flux of the beam. For a realistic power-law distribution of the beam, the main part of the beam flux is given by electrons with energy close to the low-energy cutoff of this distribution. For these reasons and for simplicity, we consider the monoenergetic beam in our model.

We used two models for estimating  $n_R$ . First, following Norman & Smith (1978), the number of runaway electrons can be estimated as

$$\alpha = \frac{n_R}{n_e} = \frac{1}{2} \exp \left[ -\frac{1}{2} \left( \sqrt{\frac{\mathcal{E}_D}{\mathcal{E}}} - \frac{\mathcal{E}}{\mathcal{E}_D} \right)^2 \right], \quad (2)$$

where  $\mathcal{E}/\mathcal{E}_D = n_B v_B / n_e v_{T_e}$  (see Karlický et al. 2004; Xu et al. 2005, for definition of the electric field  $\mathcal{E}$  generated by the electron beam and the Dreicer electric field  $\mathcal{E}_D$ ), and  $v_{T_e}$  stands for the thermal velocity of the background electrons. In the second model we assume that the return current is formed by a fixed rel-

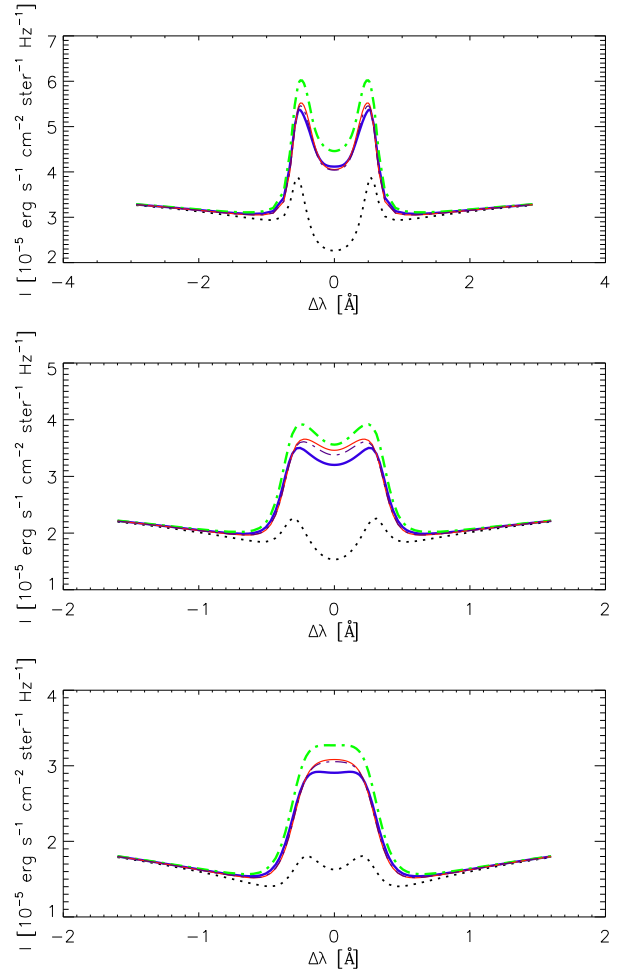


**Fig. 2.** Same as Fig. 1 plus including collisions with return-current electrons. The value of  $\alpha$  is given by Eq. (2).

ative number of background electrons everywhere in the upper chromosphere:

$$\alpha = \frac{n_R}{n_e} = \text{const.} \quad (3)$$

In this model,  $\alpha$  is obtained by averaging the values from the previous model over the Balmer line formation layers. The resulting value for each beam flux can be found in Table 1.

The normalized energy distribution of electrons can be locally expressed in the form

$$f(E) dE = [c_M f_M(E) + c_B \delta(E - E_B) + c_R \delta(E - E_R)] dE, \quad (4)$$

where  $E_R = m_e v_R^2 / 2$  is the return-current energy and  $c_i$  stands for the normalization coefficients (i.e.,  $c_R = n_R / (n_M + n_B + n_R)$ , etc.). The index M stands for the background electrons (without the runaway ones), and they obey the Maxwell-Boltzmann energy distribution.

### 3. Hydrogen-electron collisions

To take the effect of the beam/return current into account, we have to calculate all the electron-hydrogen excitation rates, the rates of ionization by electron impacts, and the rates of the inverse processes. We use the data for total collisional cross-sections for the bound-bound and bound-free transitions by

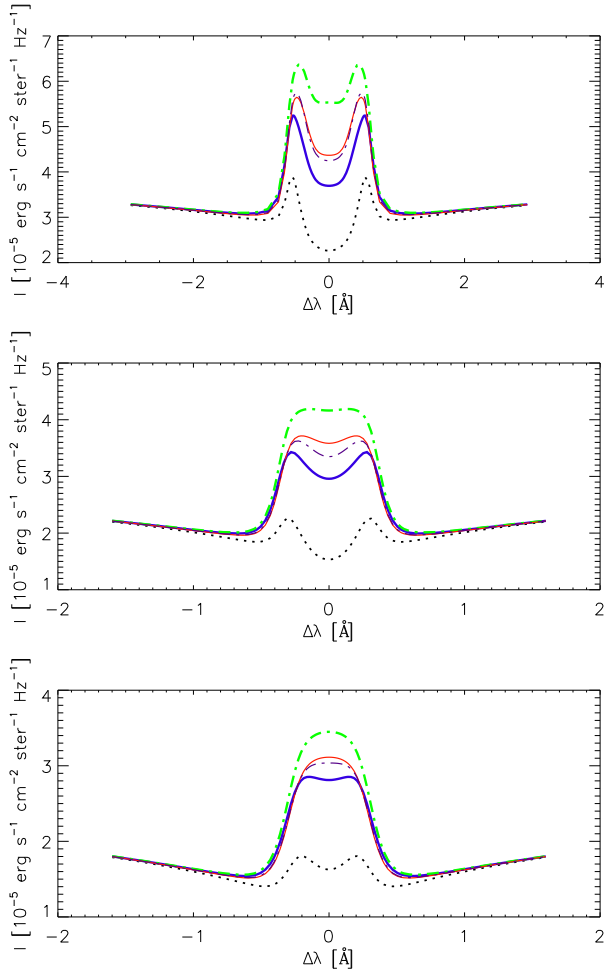


**Fig. 3.** Same as Fig. 1 plus including collisions with return-current electrons. The value of  $\alpha$  is constant along whole beam trajectory.

Janev & Smith (1993), retrieved through the GENIE database (<http://www-amdis.iaea.org/GENIE/>). We do not consider any atomic polarization or angular dependence of the collisional processes in this work. The excitation or deexcitation rate of the  $n \rightarrow m$  transition between the two shells can be calculated using the common formula

$$C_{nm} = n_e \int_0^\infty dE \sqrt{\frac{2E}{m_e}} f(E) \sigma_{nm}(E), \quad (5)$$

where  $\sigma_{nm}(E)$  is the total cross-section of  $n \rightarrow m$  at impact energy  $E$ , and  $f(E)$  is electron energy distribution (4). The cross-sections for deexcitation  $m \rightarrow n$  ( $m > n$ ) were calculated using the  $n \rightarrow m$  cross section and the principle of detailed balance (e.g., Jefferies 1968),

$$\sigma_{mn}(E) = \frac{g_n}{g_m} \frac{E + E_{nm}}{E} \sigma_{nm}(E + E_{nm}), \quad (6)$$

where  $E_{nm}$  is the excitation threshold of the transition and  $g_{n/m}$  the statistical weight of the given level.

The rates of the inverse process of ionization by an electron impact, the three-body recombination  $e + e + p \rightarrow \text{H I} + e$ , must be treated separately due to the nonthermal nature of the problem. Using the arguments of detailed balance (Fowler 1955; Jefferies 1968) in the quasi-classical approximation of the

electron-hydrogen collisions, one can derive a formula for the recombination rate. Let us consider the ionization of level  $n$  with the ionization energy  $E_n$  by an electron with energy  $E_i$ . Once cross-section  $S_{nc}(E_i, E_a) \equiv \partial \sigma_{nc} / \partial E_a$  of the encounter after which we find the two electrons with energies  $E_a$  and  $E_b = E_i - E_n - E_a$  is known, one can write the total recombination rate as

$$C_{cn} = L \int_0^\infty dE_a \int_0^\infty dE_b \frac{f(E_a)f(E_b)}{\sqrt{E_a E_b}} E_i S_{nc}(E_i, E_a), \quad (7)$$

where  $L = n_e^2 n^2 h^3 / 16 \pi m_e^2 \approx 6.97 \times 10^{-27} n_e^2 n^2$  in cgs units, and  $h$  stands for the Planck constant. The expression (7) can be reduced to the well-known expression  $C_{cn}^{\text{Thermal}} = 2.06 \times 10^{-16} n^2 T^{-3/2} n_e \exp(E_n/k_B T) C_{nc}^{\text{Thermal}}$  in the particular case of Maxwell-Boltzmann distribution, where  $T_e$  is the temperature of electrons and  $k_B$  the Boltzmann constant. For the cross section  $S_{nc}$  we used the approximate data of Omidvar (1965) at lower energies and the classical formula of Thomson (1912) at high energies. In our case, the electron energy distribution function given by (4) leads to 9 terms that contribute to the recombination rates. We verified numerically that, in all our models, the rates of three-body recombination involving the nonthermal electrons of the return current are more than one order of magnitude below the rates of the same processes involving the thermal electrons. Our tests show that neglecting the nonthermal three-body recombination affects the resulting profiles in a very negligible way. The three-body recombinations involving the beam electrons are completely negligible since their rates are several orders of magnitude below the thermal ones. Thus, we took only the thermal term containing  $m^2 f_M(E_a) f_M(E_b)$  into account.

## 4. Results

We calculated the NLTE radiative transfer for a 5-level plus continuum hydrogen using the semiempirical 1D plane-parallel flare model F1 (Machado et al. 1980) in which the temperature structure was kept fixed; in this way, we found the differential effects on the H $\alpha$ , H $\beta$ , and H $\gamma$  lines (cf. Kašparová & Heinzel 2002). We used the preconditioned equations of statistical equilibrium (Rybicki & Hummer 1991) and solved the coupled system of NLTE equations by the accelerated lambda iteration (ALI) method. For further details, see Heinzel (1995). We found the equilibrium state for several beam fluxes with or without the return current. The initial beam fluxes chosen in our calculations were:  $\mathcal{F}_1 = 4 \times 10^{11}$ ,  $6 \times 10^{11}$ ,  $8 \times 10^{11}$ , and  $1 \times 10^{12}$  erg cm $^{-2}$  s $^{-1}$ . If the fluxes were lower, the number of runaway electrons would decrease fast and their energy would exceed the beam energy in most depths. This gives a limit for using of this simple model. Higher fluxes, on the other hand, would be unrealistic. The initial energy of beam electrons was set to  $E_0 = 10$  keV.

In Fig. 1, there are first three Balmer line profiles that result from the nonthermal bombardment by the primary beam. The effects of return current were completely ignored. In this sense, these calculations are similar to the ones of Fang et al. (1993) and Kašparová & Heinzel (2002). In spite of their probably limited physical relevance, these profiles are useful for demonstrating the effects of return currents in the more appropriate models that follow. Figure 2 shows the situation where  $\alpha$  is calculated using Eq. (2); i.e., the relative number of runaway return-current electrons is calculated at each depth in the atmosphere. Finally, in Fig. 3, there are profiles for the model with  $\alpha$  constant along the atmosphere. In the layers of Balmer line formation,  $\alpha$  remains approximately constant and its mean values are shown in

**Table 1.** The properties of the return currents.  $\mathcal{F}_1$  stands for the initial flux of the 10 keV beam,  $\alpha$  is the mean relative number of runaway return-current electrons in the Balmer lines formation region, and  $E_R$  stands for the typical energy of the return-current electrons in these layers. Both  $\alpha$  and  $E_R$  are average quantities which can roughly characterize the return-current properties in the region of interest.

$\mathcal{F}_1 [10^{11} \text{ erg cm}^{-2} \text{ s}^{-1}]$	$\alpha$	$E_R [\text{eV}]$
4	0.01	100
6	0.05	14
8	0.11	6
10	0.16	3.8

Table 1. Comparing Fig. 1 with Figs. 2 and 3, one can see that the effect of return current is very significant: All three lines show a prominent increase emission in the line center.

In the region of Balmer line formation, the energy of the return current can be close to the excitation threshold of  $n \geq 3$  levels of hydrogen, and it remains approximately constant along an extended trajectory. The beam is finally stopped on a very short path. The overall path of the beam is, however, sensitive to the initial energy of the beam. In order to model the beam propagation and line formation accurately, one has to interpolate the original F1 model of Machado et al. (1980) by a number of grid points in the layers of the Balmer line formation. Since the return-current energy and density are sensitive to the beam flux (see Table 1), the resulting variation of the nonthermal collisional rates leads to a significant variation in line profiles. For both models under consideration, a maximum emission is found for the beam flux of  $6 \times 10^{11} \text{ erg cm}^{-2} \text{ s}^{-1}$ , although the resulting profiles from these models differ slightly from each other. In contrast to the case of  $4 \times 10^{11} \text{ erg cm}^{-2} \text{ s}^{-1}$ , for which we found the least emission among the studied flux intervals, the return-current density is higher by a factor of 5. It leads to a significant increase in nonthermal excitation rates. The disagreement of the profiles at fluxes below  $6 \times 10^{11} \text{ erg cm}^{-2} \text{ s}^{-1}$  is the result of the significant dependency of  $\alpha$  on the beam flux and atmospheric depth. The values of  $\alpha$  at low fluxes (shown in the Table 1) are only a rough approximation for the Balmer line formation layers, and the model with  $\alpha = \text{const.}$  seems to be less accurate than the one given by Eq. (2). On the other hand, good correspondence between the models is found for high fluxes. In this case, the variation in  $\alpha$  is less sensitive to the beam flux and does not strongly vary with atmospheric depth. Then, the  $\alpha = \text{const.}$  model seems to give the appropriate results. The reason the higher beam fluxes lead to a lower emission in the lines is that the energy of the return current is not sufficient to excite hydrogen atoms as can be seen in Table 1.

## 5. Conclusions and outlook

In this paper we used a simple model of the 10 keV electron beam propagating in the chromosphere. We used two different models of the return-current formation and calculated the differential effect on the profiles of the hydrogen  $H\alpha$ ,  $H\beta$ , and  $H\gamma$  lines of the semiempirical F1 model.

The return-current flux only depends on the total flux of the beam. For a realistic power-law distribution of the beam, the main part of the beam flux is given by electrons with energy close to the low-energy cutoff of this distribution. Therefore, for simplicity we used the monoenergetic beam in our model. Moreover, the excitation and ionization cross-sections of low-

energy return-current electrons are larger than those for beam electrons, which makes the return-current effects on line core formation stronger. Taking high-energy beam electrons into account (i.e. using power-law distribution) would lead to increased emission in the line wings due to penetration of those electrons into the deeper atmospheric layers. However, the total flux of the beam in these layers is significantly lower than the initial beam flux, and the return current and corresponding effects are also strongly reduced.

Even our simple model shows that the effect of return current is very important for future study of the hydrogen lines formation since the energy of the return current can be expected to be on the order of the excitation threshold energies of upper hydrogen levels, for which the excitation cross-sections are high. Moreover, the fluxes  $\Phi$  are high enough to excite a sufficient number of atoms. As shown by Karlický et al. (2004), the collisional rates from the nonthermal collisions can dominate the collisional rates in the Balmer line formation regions. The two models used in this work lead to similar results for higher energy fluxes, but the result differs for lower fluxes. The excitation threshold effects seem to play an important role for higher fluxes, but they are very likely only a consequence of the monoenergetic model we used. The difference between the two models shows the used approximations to be incompatible for lower fluxes, where the approximation of constant  $\alpha$  is not applicable. A detailed description of the energy distribution of the return-current electrons would lead to more realistic line intensities. This complex issue will be subject of a forthcoming paper, which will also study the impact polarization of the Balmer lines.

*Acknowledgements.* This work was partially supported by the grant 205/06/P135 of the Grant Agency of the Czech Republic, partially by the grant IAA300030701 of the Grant Agency of the Academy of Sciences of the Czech Republic, and partially by the project LC06014 Center for Theoretical Astrophysics.

## References

- Canfield, R. C., Gunkler, T. A., & Ricchiazzi, P. J. 1984, *ApJ*, 282, 296
- Emslie, A. G. 1978, *ApJ*, 224, 241
- Fang, C., Henoux, J. C., & Gan, W. Q. 1993, *A&A*, 274, 917
- Fowler, R. H. 1955, *Statistical mechanics* (Cambridge University Press)
- Hawley, S. L. & Fisher, G. H. 1994, *ApJ*, 426, 387
- Heinzel, P. 1995, *A&A*, 299, 563
- Janev, R. K. & Smith, J. J. 1993, in *Atomic and plasma-material interaction data for fusion*, Vol. 4, 1–180
- Jefferies, J. T. 1968, *Spectral line formation* (A Blaisdell Book in the Pure and Applied Sciences, Waltham, Mass.: Blaisdell, 1968)
- Karlický, M. 1997, *Space Sci. Rev.*, 81, 143
- Karlický, M. & Hénoux, J.-C. 2002, *A&A*, 383, 713
- Karlický, M., Kašparová, J., & Heinzel, P. 2004, *A&A*, 416, L13
- Kašparová, J. & Heinzel, P. 2002, *A&A*, 382, 688
- Machado, M. E., Avrett, E. H., Vernazza, J. E., & Noyes, R. W. 1980, *ApJ*, 242, 336
- Norman, C. A. & Smith, R. A. 1978, *A&A*, 68, 145
- Omidvar, O. 1965, *Phys. Rev.*, 140, A26
- Rowland, H. L. & Vlahos, L. 1985, *A&A*, 142, 219
- Rybicki, G. B. & Hummer, D. G. 1991, *A&A*, 245, 171
- Štěpán, J., Heinzel, P., & Sahal-Bréchet, S. 2007, *A&A*, 465, 621
- Thomson, J. J. 1912, *Phil. Mag.*, 23, 449
- van den Oord, G. H. J. 1990, *A&A*, 234, 496
- Xu, Z., Hénoux, J.-C., Chambe, G., Karlický, M., & Fang, C. 2005, *ApJ*, 631, 618